

# Chemical Inhibition of Acetyl-CoA Carboxylase Induces Growth Arrest and Cytotoxicity Selectively in Cancer Cells

Annelies Beckers, Sophie Organe, Leen Timmermans, Katryn Scheys, Annelies Peeters, Koen Brusselmans, Guido Verhoeven, and Johannes V. Swinnen

Laboratory for Experimental Medicine and Endocrinology, Gasthuisberg, K.U.Leuven, Leuven, Belgium

## Abstract

**Development and progression of cancer is accompanied by marked changes in the expression and activity of enzymes involved in the cellular homeostasis of fatty acids. One class of enzymes that play a particularly important role in this process are the acetyl-CoA carboxylases (ACC). ACCs produce malonyl-CoA, an intermediate metabolite that functions as substrate for fatty acid synthesis and as negative regulator of fatty acid oxidation. Here, using the potent ACC inhibitor soraphen A, a macrocyclic polyketide from myxobacteria, we show that ACC activity in cancer cells is essential for proliferation and survival. Even at nanomolar concentrations, soraphen A can block fatty acid synthesis and stimulate fatty acid oxidation in LNCaP and PC-3M prostate cancer cells. As a result, the phospholipid content of cancer cells decreased, and cells stopped proliferating and ultimately died. LNCaP cells predominantly died through apoptosis, whereas PC-3M cells showed signs of autophagy. Supplementation of the culture medium with exogenous palmitic acid completely abolished the effects of soraphen A and rescued the cells from cell death. Interestingly, when added to cultures of premalignant BPH-1 cells, soraphen A only slightly affected cell proliferation and did not induce cell death. Together, these findings indicate that cancer cells have become dependent on ACC activity to provide the cell with a sufficient supply of fatty acids to permit proliferation and survival, introducing the concept of using small-molecule ACC inhibitors as therapeutic agents for cancer. [Cancer Res 2007;67(17):8180–7]**

## Introduction

Development and progression of cancer is typically accompanied by changes in the expression and activation of proteins involved in the synthesis, transport, and metabolism of fatty acids (1, 2). The protein that has been studied most extensively in this respect is fatty acid synthase (FASN), the enzyme that catalyzes all terminal steps in the synthesis of saturated long-chain fatty acids (3). Overexpression of this enzyme is found already in the earliest stages of tumor development and becomes more pronounced as the tumor progresses (4–7). To gain more insight into the role of FASN overexpression in cancer cells and to explore its potential as a target for antineoplastic intervention, several chemical compounds, including cerulenin, c75, and Orlistat, were used as FASN inhibitor (8–15). Although these inhibitors are not monospecific

and are effective only at micromolar concentrations, inhibition of FASN invariably resulted in growth arrest and induced cell death selectively in cancer cells (8–15). Similar observations were made when FASN was down-regulated by RNA interference (16).

Another class of enzymes that play a key role in the cellular homeostasis of fatty acids are the acetyl-CoA carboxylases (ACC). ACCs are biotin-containing enzymes that catalyze the carboxylation of acetyl-CoA to form malonyl-CoA. In humans, there are two ACC isoforms, ACC1 ( $M_r = 265,000$ ) and ACC2 ( $M_r = 280,000$ ), that are encoded by two separate genes (17). ACC1 is mainly cytosolic and fuels the malonyl-CoA pool that is used as  $C_2$ -unit donor for *de novo* synthesis of long-chain fatty acids by FASN and for subsequent chain elongation. ACC2 is associated with the mitochondria and regulates a second pool of malonyl-CoA that governs fatty acid oxidation through inhibition of carnitine palmitoyltransferase I, the enzyme that facilitates the entry of long-chain fatty acids into mitochondria for  $\beta$ -oxidation (4, 18). Both enzymes show a high degree of sequence homology and are similarly regulated through a combination of transcriptional, translational, and posttranslational mechanisms. In cancer cells, both ACC isoforms have been shown to be overexpressed coordinately with FASN (4, 5) and are activated downstream from mutations in tumor suppressors, including LKB1 and BRCA1 (19–22). However, treatment of cancer cells with 5-(tetradecyloxy)-2-furoic acid (TOFA), a classic inhibitor of ACC, did not affect cell proliferation and failed to induce apoptosis (23, 24). Preincubation of cells with TOFA even protected cells from FASN inhibitor-induced cytotoxicity. On the basis of these data, it was concluded that accumulation of malonyl-CoA is the main mediator of the cytotoxic effects of FASN inhibition and ACC was abandoned as a potential target for cancer intervention.

Recently, two studies have shown that silencing of ACC1 by RNA interference causes growth inhibition and induces cell death almost to the same extent as observed after silencing of FASN gene expression (25, 26). These findings suggest that apart from malonyl-CoA accumulation, inhibition of lipogenesis per se may cause cancer cell death and that ACC may be a target for antineoplastic therapy after all. However, up to now, no reports have been published on the use of chemical ACC inhibitors to block the proliferation of cancer cells, nor could in the ACC1 knockdown experiment the involvement of local increases in malonyl-CoA levels (due to compensatory activation of ACC2) be excluded.

Here, we report on the use of a highly potent ACC inhibitor soraphen A. Soraphen A is a natural macrocyclic polyketide originally isolated from the myxobacterium *Sorangium cellulosum*. It displays potent antifungal activities that have been attributed to its ability to bind to the biotin carboxylase domain dimer interface of eukaryotic ACCs, thereby disrupting the oligomerization of the enzyme and inhibiting its activity (27–32). Soraphen A has been shown to inhibit also human ACCs in an isoform-nonspecific

**Requests for reprints:** Johannes V. Swinnen, Laboratory for Experimental Medicine and Endocrinology, Gasthuisberg, O&N1, K.U.Leuven, Herestraat 49 bus 902, B-3000 Leuven, Belgium. Phone: 32-16-33-05-33; Fax: 32-16-34-59-34; E-mail: johan.swinnen@med.kuleuven.be.

©2007 American Association for Cancer Research.  
doi:10.1158/0008-5472.CAN-07-0389

manner (31). We show that sorafenib, at nanomolar concentrations, blocks lipogenesis and enhances fatty acid oxidation in prostate cancer cells. Cancer cells stop proliferating and ultimately die. When sorafenib was added to cultures of premalignant cells, no cytotoxic effects were observed. These findings suggest that cancer cells have become dependent on ACC activity to provide the cell with sufficient fatty acids to proliferate and survive. To the best of our knowledge, this is the first report to introduce the concept of using ACC inhibitors as therapeutic agents for cancer.

## Materials and Methods

**Cell lines and cell culture.** LNCaP and BPH-1 cells, obtained from the American Type Culture Collection, were maintained at 37°C in a humidified incubator with a 5% CO<sub>2</sub>/95% air atmosphere in RPMI 1640 supplemented with 10% FCS (Invitrogen). For experiments on the effects of R1881 (Perkin-Elmer Life Sciences) on LNCaP cells, cells were seeded in medium supplemented with 5% charcoal-treated serum as described previously (33). For routine maintenance of BPH-1 cells, 70 nmol/L testosterone and 1% insulin-transferrin-selenium mixture (Invitrogen) was added to the culture medium. PC-3M-luc-C6 cells (further referred to as PC-3M) were obtained from Xenogen Corporation and were maintained at 37°C in a 5% CO<sub>2</sub>/95% air atmosphere in MEM supplemented with 10% FCS, 1% sodium pyruvate, 1% MEM vitamin solution, and 1% MEM nonessential amino acids (Invitrogen). Nonmalignant human skin fibroblasts were cultured as described previously (25). Sorafenib, purified from the myxobacterium *S. cellululosum*, was provided by Drs. Klaus Gerth and Rolf Jansen (Hemholtz Zentrum für Infektionsforschung GmbH, Braunschweig, Germany).

**[2-<sup>14</sup>C]acetate incorporation assay and quantitation of lipid species.** Cells were seeded at a density of  $4 \times 10^5$  per dish (LNCaP) or  $1 \times 10^5$  per dish (PC-3M and BPH-1) and treated with sorafenib or vehicle (ethanol) as indicated. Etomoxir (Sigma Chemical) was added to a final concentration of 10 µg/mL to prevent oxidation of fatty acids. Twenty hours after treatment, [2-<sup>14</sup>C]acetate (57 mCi/mmol; 1 µCi/6-cm dish; Amersham International plc) was added to the cultures. Four hours later, cells were washed with PBS, scraped, and resuspended in 0.9 mL PBS (Invitrogen). Lipids were extracted using the Bligh-Dyer method (33). <sup>14</sup>C incorporation into lipids was measured by scintillation counting and normalized for sample protein content. To analyze <sup>14</sup>C incorporation into different lipid classes, lipids were separated by TLC and were quantitated using a Phosphor Imager screen (Molecular Dynamics; ref. 33). Quantitation of phospholipids and free cholesterol was carried out as described previously (34, 35).

**Measurement of fatty acid oxidation.** Cells were seeded at a density of  $4 \times 10^5$  (LNCaP) or  $1 \times 10^5$  (PC-3M and BPH-1) in T25 flasks and treated with sorafenib as indicated. After 24 h, cells were incubated with [1-<sup>14</sup>C]palmitic acid (54 mCi/mmol; 0.5 µCi/6-cm flask; Sigma), complexed to fatty acid-free bovine serum albumin (BSA; see below). Flasks were made airtight by using stopper tops. After 6 h, 200 µL KOH (10 N) was added with a syringe to a center well containing a folded Whatman filter paper. Subsequently, 1 mL of 12% perchloric acid was added to the medium through the stopper tops using a syringe, without touching the cells, to release the labeled CO<sub>2</sub> from the medium. The flasks were placed for a minimum of 1 h at 37°C to trap labeled CO<sub>2</sub>. Finally, the filter paper was removed and transferred to a scintillation vial for radioactivity counting.

**Proliferation/cytotoxicity assays and fluorescence-activated cell sorting analysis.** At the indicated time points after treatment, cells were collected and cell number and viability were determined using a trypan blue dye exclusion assay (14). For experiments on the mechanism of cell death, 50 µmol/L *N*-benzoyl-oxycarbonyl-Val-Ala-Asp-fluoromethylketone (z-VAD-fmk; Sigma) or 10 mmol/L 3-methyladenine (Sigma) was added to the culture medium of cells 24 h (for z-VAD-fmk) or 48 h (for 3-methyladenine) after treatment with sorafenib or vehicle. Palmitic acid (Sigma) was dissolved in ethanol at a final concentration of 5 mmol/L and complexed to fatty acid-free BSA (Sigma) by adding 4 volumes of a 4% BSA solution in 0.9% NaCl to 1 volume of palmitic acid (5), and incubated at 37°C for 1 h to obtain a 1 mmol/L stock solution of BSA-complexed palmitic acid. This complex was added to the culture medium at a concentration of 75 µmol/L and effects on cell death were examined by trypan blue staining. Cell proliferation was also quantitated using the bromodeoxyuridine (BrdUrd) labeling and detection kit III (Roche Diagnostics) at 72 h after treatment. For fluorescence-activated cell sorting (FACS) analysis, cells were trypsinized and fixed in ice-cold 70% ethanol for 1 h, 96 h after treatment with sorafenib. After fixation, cells were washed twice with PBS containing 0.05% Tween 20 and resuspended in PBS containing 0.05% Tween 20, 0.5 mg/mL propidium iodide (Sigma), and 1 mg/mL RNase A (Sigma). Analysis of samples was done using the CellQuest and Modfit software on a FACSort cytometer (Becton Dickinson).

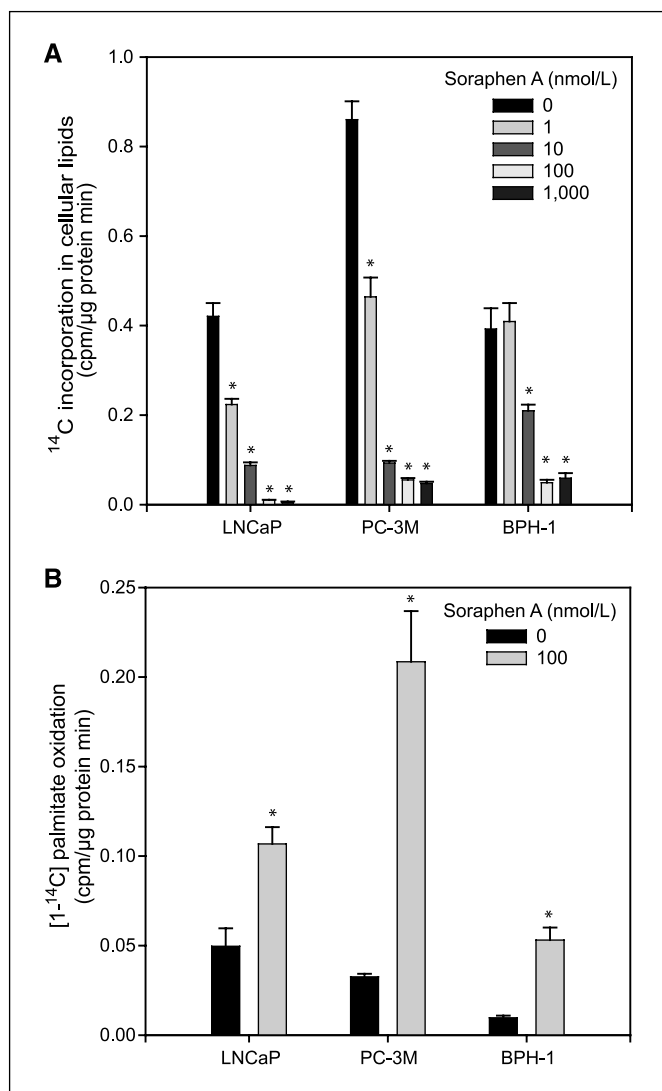


**Figure 1.** Sorafenib decreases the ability of cancer cells to synthesize fatty acids and increases fatty acid oxidation. **A**, cells were seeded in a 6-cm dish at a density of  $4 \times 10^5$  per dish (LNCaP) or  $1 \times 10^5$  per dish (PC-3M, BPH-1). The next day, cells were treated with sorafenib, as indicated, and etomoxir (final concentration, 10 µg/mL). After 20 h, cells were exposed to [2-<sup>14</sup>C]acetate for 4 h. Cellular lipids were extracted and [2-<sup>14</sup>C]acetate incorporation was measured by scintillation counting. Results are representative of three independent experiments. Columns, means of triplicate measurements; bars, SE. \*,  $P < 0.05$ , significantly different from control (0 nmol/L). **B**, cells were seeded in a 6-cm dish at a density of  $4 \times 10^5$  per dish (LNCaP) or  $1 \times 10^5$  per dish (PC-3M, BPH-1). The next day, cells were treated with sorafenib as indicated. After 24 h, [1-<sup>14</sup>C]palmitic acid was added for 6 h and the incorporation of radiolabel into CO<sub>2</sub> was measured. Results are representative of three independent experiments. Columns, means of triplicate measurements; bars, SE. \*,  $P < 0.05$ , significantly different from control (0 nmol/L).

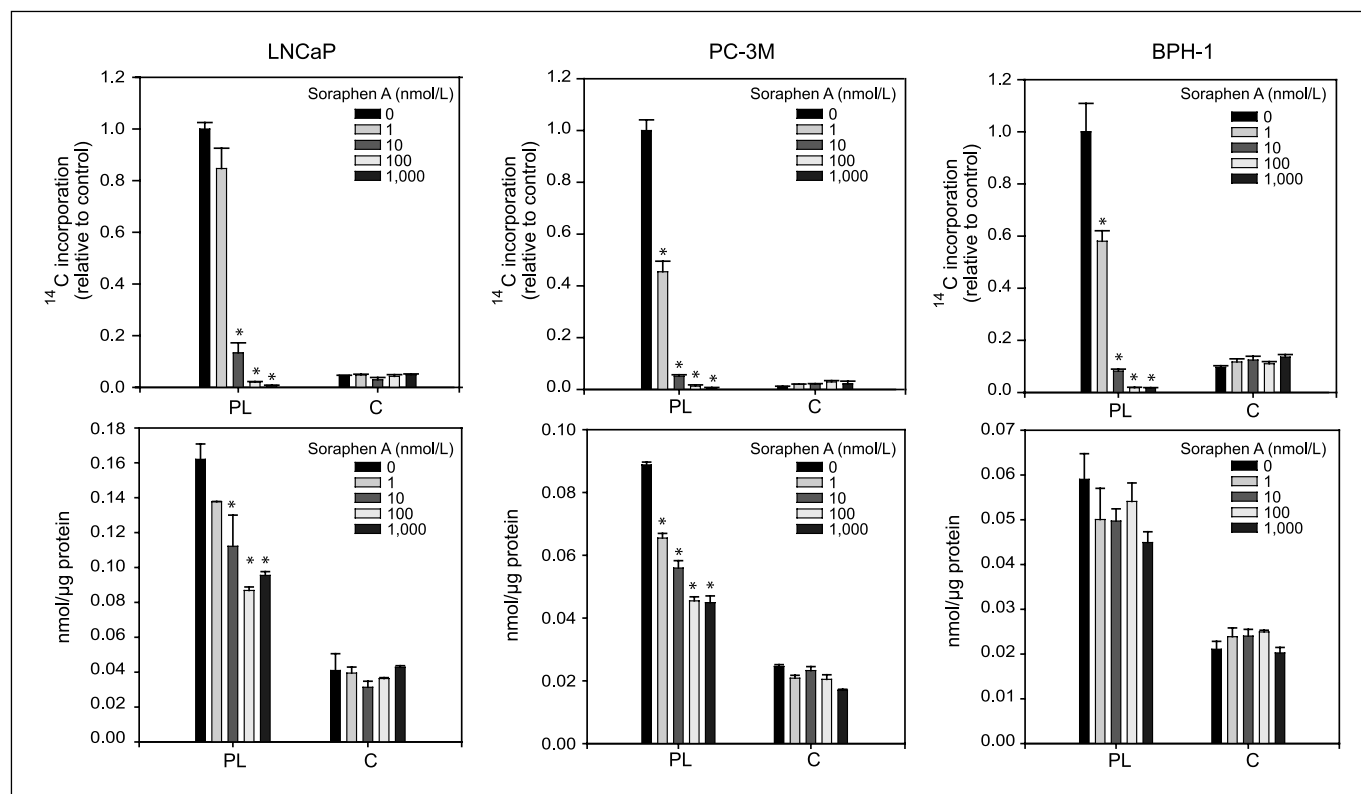


**Figure 2.** Sorafenib decreases the total amount of phospholipids in cancer cells. *Top panels*, cells were treated with sorafenib A and  $[2-^{14}\text{C}]$ acetate as in Fig. 1. After lipid extraction, the different lipid species were separated by TLC and quantitated by Phosphor Imaging. PL, phospholipids; C, cholesterol. Results are representative of three independent experiments. Columns, means of triplicate measurements; bars, SE. \*,  $P < 0.05$ , significantly different from control (0 nmol/L). *Bottom panels*, cells were seeded in a 6-cm dish at a density of  $4 \times 10^5$  per dish (LNCaP) or  $1 \times 10^5$  per dish (PC-3M, BPH-1). The next day, cells were treated with sorafenib A as indicated. After 96 h, cellular lipids were extracted and total amount of phospholipids and free cholesterol was measured (34, 35). Results are representative of three independent experiments. Columns, means of triplicate measurements; bars, SE. \*,  $P < 0.05$ , significantly different from control (0 nmol/L).

**Detection of apoptosis.** Cells were plated in 6-cm dishes and treated with sorafenib A as indicated. After 96 h, Hoechst 33342 (Sigma) was added to the culture medium of living cells; fragmentation of the nucleus into oligonucleosomes and chromatin condensation were detected by fluorescence microscopy using a filter for Hoechst 33342 (365 nm). Apoptosis was also determined with an Annexin V-FITC/Propidium Iodide Apoptosis detection kit (Clontech Laboratories, Inc.) according to the manufacturer's protocol. The cells were washed and subsequently incubated with Annexin V-FITC for 15 min at room temperature and counterstained with propidium iodide (final concentration 1  $\mu\text{g}/\text{mL}$ ). Afterward, apoptosis was analyzed by fluorescence microscopy using a dual-filter set for FITC and propidium iodide.

**Detection of autophagy.** To study the formation of autophagic vacuoles, the localization of LC3, a specific marker of autophagosomes, was monitored. LC3 was expressed as an amino-terminal fusion with green fluorescent protein (EGFP) using Oligofectamine (Invitrogen) for LNCaP cells and FuGene (Roche) for PC-3M cells. The plasmid encoding EGFP-LC3 was provided by Prof. Dr. Tamotsu Yoshimori (Department of Cell Genetics, National Institute of Genetics, Shizuoka-ken, Japan; ref. 36). Cells were subsequently treated with sorafenib A or vehicle for 96 h. As a positive control, cells were washed thrice with PBS and incubated with HBSS (Invitrogen) for 6 h. Autophagy was analyzed by fluorescence microscopy using a filter set for EGFP. Autophagic vacuoles were also visualized by labeling with the fluorophore monodansylcadaverine (Sigma). Cells were incubated with 0.05 mmol/L monodansylcadaverine in PBS at  $37^\circ\text{C}$  for 10 min before fixation using a 4% paraformaldehyde solution in PBS for 10 min at room temperature (37–39). Intracellular monodansylcadaverine was analyzed by fluorescence microscopy (excitation wavelength 380 nm, emission filter 525 nm).

**Immunoblotting.** For Western blot analysis of the cleavage of poly(ADP-ribose) polymerase (PARP) or LC3, cells were seeded at a density of  $4 \times 10^5$  (LNCaP) or  $1 \times 10^5$  cells (PC-3M) per 6-cm dish and treated with sorafenib A or vehicle. After 96 h, cells were washed with PBS and lysed in a reducing NuPage sample loading buffer (Invitrogen). As previously described (33), equal amounts of protein were separated on NuPage gels (Invitrogen) and processed for immunoblot analysis for cleaved PARP (Cell Signaling Technology, Inc.) or LC3 (Santa Cruz Biotechnology), which recognizes both the cytosolic LC3-I as well as the membrane-associated LC3-II form. Equal loading of proteins was confirmed by immunoblotting for  $\alpha$ -tubulin (Cell Signaling Technology).

**Statistics.** Statistical analyses were done using one-way ANOVA with Tukey's multiple comparison test;  $P < 0.05$  was considered statistically significant. All data are means  $\pm$  SE.

## Results

**Sorafenib A decreases fatty acid synthesis and increases fatty acid oxidation in prostate cell lines.** LNCaP and PC-3M prostate cancer cells and premalignant BPH-1 cells were treated with increasing concentrations of sorafenib A. Fatty acid synthesis was measured by exposing the cells for 4 h to  $[2-^{14}\text{C}]$ acetate after pretreatment with etomoxir, an irreversible inhibitor of carnitine *O*-palmitoyltransferase-1 (40) to block fatty acid oxidation. Cellular lipids were extracted and the incorporation of  $[2-^{14}\text{C}]$ acetate into cellular lipids was measured using scintillation counting. Figure 1A shows that in all cell lines, sorafenib A treatment led to a dose-dependent decrease in lipid production. Inhibition of  $[2-^{14}\text{C}]$ acetate

incorporation was already seen at concentrations as low as 1 nmol/L and was maximal at ~100 nmol/L (Fig. 1A).

Fatty acid oxidation was measured by adding [1-<sup>14</sup>C]palmitic acid to the medium. Conversion of [1-<sup>14</sup>C]palmitic acid to <sup>14</sup>C-labeled CO<sub>2</sub> was measured by scintillation counting. Sorafenib A enhanced the oxidation of fatty acids by 2- to 7-fold, depending on the cell line (Fig. 1B).

**Sorafenib A decreases the amount of phospholipids of prostate cancer cells.** The major end product of fatty acids in cancer cells are phospholipids (41). Therefore, the effect of sorafenib A on this lipid class was studied with [2-<sup>14</sup>C]acetate. In all cell lines tested, sorafenib A induced a dramatic dose-dependent decrease in *de novo* synthesis of phospholipids (Fig. 2, top panels). Already at a concentration of 10 nmol/L sorafenib A, labeling of phospholipids had dropped to 13% of control levels. Labeling of cholesterol was unaffected. Quantitation of total amounts of phospholipids revealed a dose-dependent decrease of phospholipids down to 50% to 60% of control in prostate cancer cells. Interestingly, in BPH-1 cells, no significant changes in phospholipid levels could be observed (Fig. 2, bottom panels). Levels of cholesterol were unaffected in all cell lines.

**Sorafenib A inhibits proliferation and induces cell death selectively in cancer cells.** To explore the effect of sorafenib A on cell proliferation and cell survival, cells were collected at different time points after treatment with sorafenib A, stained with trypan blue, and counted. Treatment of LNCaP and PC-3M cells with sorafenib A resulted in a dose-dependent decrease in the number of viable cells. By contrast, BPH-1 cells (Fig. 3, top panels) and nonmalignant human skin fibroblasts (data not shown) continued to proliferate normally.

These results were confirmed by BrdUrd incorporation (data not shown); treatment of cells with sorafenib A for 72 h resulted in a significant decrease in proliferation in LNCaP and PC-3M prostate cancer cells. In the BPH-1 control cell line, effects of sorafenib A were less prominent.

Furthermore, trypan blue staining indicated sorafenib A to cause cell death in the LNCaP and PC-3M cell line. The percentage of dead cells increased dose-dependently, reaching 50% and 30% in LNCaP and PC-3M cells, respectively, at 120 h after treatment with 1 μmol/L sorafenib A (Fig. 3, bottom panels). In the BPH-1 (Fig. 3, bottom panels) and nonmalignant fibroblasts (data not shown), however, there was no evidence for an increase in cell death caused by sorafenib A.

These effects of sorafenib A were confirmed by FACS analysis. As shown in Table 1, sorafenib A induced an accumulation of cancer cells in the G<sub>0</sub>-G<sub>1</sub> phase and in the sub-G<sub>1</sub> fraction and caused a marked reduction of cells in the S and the G<sub>2</sub>-M phase. In BPH-1 cultures, no increase in sub-G<sub>1</sub> cells was observed and the effects on the various phases of the cell cycle were much less pronounced than in the cancer cell cultures.

**Sorafenib A induces apoptosis in LNCaP cells and autophagy in PC-3M cells.** To test whether sorafenib A-treated cancer cells die through induction of apoptosis, cells were stained with the nuclear dye Hoechst 33342. As illustrated in Fig. 4A, LNCaP cells treated with 100 nmol/L sorafenib A displayed DNA condensation and nuclear fragmentation, which are typical hallmarks of apoptotic cell death. The presence of apoptosis in LNCaP cells was confirmed by staining with propidium iodide (a membrane impermeable dye) and Annexin V-FITC (a protein that binds with high affinity to the phospholipid phosphatidylserine). In healthy

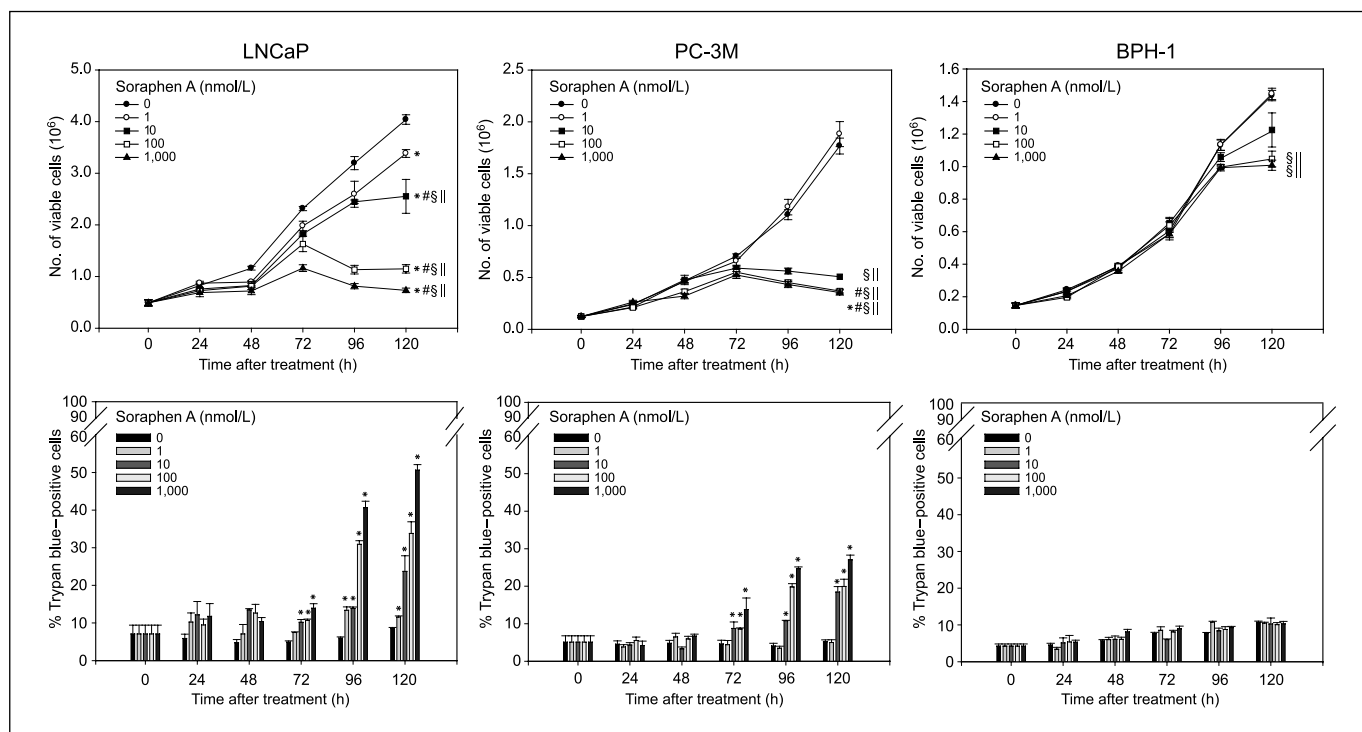


**Figure 3.** Sorafenib A inhibits growth and induces cell death of prostate cancer cells. Cells were seeded in 6-cm dishes at a density of  $4 \times 10^5$  per dish (LNCaP) or  $1 \times 10^5$  per dish (PC-3M, BPH-1). Twenty-four hours later, cells were treated with sorafenib A as indicated. At different time points after treatment, cells were collected and stained with trypan blue; the number of viable cells and percentage of dead cells were counted. Results are representative of three independent experiments. Points and columns, means of triplicate measurements; bars, SE. Top panels, viable cells. Significantly different ( $P < 0.05$ ) from control (0 nmol/L) after 48 h (\*), 72 h (#), 96 h (§), and 120 h (||). Bottom panels, dead cells. \*,  $P < 0.05$ , significantly different from control (0 nmol/L).

**Table 1.** Sorafenib A causes an accumulation of cancer cells in the G<sub>0</sub>-G<sub>1</sub> phase

Concentration (nmol/L)	Sub-G <sub>1</sub>	G <sub>0</sub> -G <sub>1</sub>	S	G <sub>2</sub> -M
<b>LNCaP</b>				
0	0.17 ± 0.09	73.24 ± 0.47	16.23 ± 0.27	10.53 ± 0.21
1	0.42 ± 0.34	73.68 ± 0.23	15.27 ± 0.14	11.05 ± 0.37
10	2.91 ± 0.30*	75.94 ± 0.53*	14.54 ± 0.45*	9.52 ± 0.17*
100	4.46 ± 0.44*	89.55 ± 0.31*	4.02 ± 0.17*	6.42 ± 0.14*
1,000	12.14 ± 1.18*	92.44 ± 0.24*	2.94 ± 0.23*	4.62 ± 0.13*
<b>PC-3M</b>				
0	0.28 ± 0.03	60.79 ± 1.13	20.99 ± 0.86	18.22 ± 0.29
1	2.51 ± 0.74	62.22 ± 1.22	19.98 ± 1.15	17.81 ± 0.07
10	2.04 ± 1.05	72.15 ± 0.58*	13.20 ± 0.54*	14.64 ± 0.56*
100	2.29 ± 0.39*	81.01 ± 0.46*	5.89 ± 0.12*	13.10 ± 0.36*
1,000	3.49 ± 0.51*	81.65 ± 0.31*	5.50 ± 0.21*	12.85 ± 0.45*
<b>BPH-1</b>				
0	1.67 ± 0.10	58.29 ± 0.64	27.85 ± 0.88	13.85 ± 0.34
1	1.42 ± 0.24	60.90 ± 0.77	25.73 ± 0.51	13.36 ± 0.41
10	1.50 ± 0.29	71.33 ± 0.61*	16.45 ± 0.57*	12.23 ± 0.92
100	0.88 ± 0.67	75.21 ± 0.31*	14.36 ± 0.31*	10.43 ± 0.28*
1,000	0.65 ± 0.65	73.40 ± 1.00*	16.41 ± 0.73*	10.19 ± 0.62*

NOTE: Cells were exposed to sorafenib A for 96 h as indicated. Cell cycle distribution of sorafenib A-treated cells was analyzed using FACS. Analysis of samples was done using the CellQuest and Modfit software on a FACSort cytometer. Sub-G<sub>1</sub> data are expressed as percentage of the total population of the cells. G<sub>0</sub>-G<sub>1</sub>, S, and G<sub>2</sub>-M data are expressed as percentage of live cells. Results are representative of three independent experiments. Data are means ± SE of triplicate values.

\*Significantly different ( $P < 0.05$ ) from control (0 nmol/L).

cells, phosphatidylserine is located almost exclusively on the inner side of the cellular membrane, whereas in apoptotic cells, it is translocated to the outer membrane leaflet. LNCaP cells stained positive for Annexin V-FITC, which reflects apoptosis. Some cells stain positive both for Annexin V-FITC and propidium iodide, a pattern reflecting membrane disruption, which is characteristic for later stages of apoptosis or necrosis (Fig. 4A). Ninety-six hours after treatment with sorafenib A, we also observed the cleavage of PARP, a major substrate of the apoptosis effector caspase-3 (Fig. 4B). As lipogenesis, cell proliferation, and cell survival of LNCaP cells are regulated by androgens (33, 42), we examined the effect of sorafenib A in the absence and presence of the synthetic androgen R1881. As expected, R1881 dose-dependently affected proliferation and survival; however, it did not influence the efficacy nor did it change the mode of cell death caused by sorafenib A, as measured by trypan blue exclusion and Hoechst staining, respectively (data not shown).

In PC-3M cells, treatment with sorafenib A for 96 h did not induce DNA condensation and nuclear fragmentation and failed to induce PARP cleavage and led to the appearance of Annexin V-FITC-negative and propidium iodide-positive cells, indicating necrosis (Fig. 4A). These data show that PC-3M cells do not undergo apoptosis. To examine alternative mechanisms of cell death, we studied the effect of sorafenib A on the localization of LC3, a marker of autophagy (Fig. 4A). During autophagy, cytosolic LC3-I is processed to form the membrane-associated LC3-II, which is

associated with autophagosomes. In PC-3M cells, transfected with a plasmid encoding EGFP-LC3, sorafenib A caused a redistribution of EGFP-LC3 into vesicular structures, as visualized by fluorescence microscopy, which is indicative of autophagic cell death. This was also confirmed by Western blotting for endogenous LC3 (Fig. 4B), revealing a major shift from the cytosolic LC3-I form to the membrane-associated LC3-II form. The involvement of autophagy was further correlated by staining with monodansylcadaverine. Under specific fixation conditions, monodansylcadaverine is retained in autophagosomal membranes (37, 39). In PC-3M cells treated with sorafenib A, monodansylcadaverine-positive structures could be visualized starting from 48 h (data not shown), reaching a maximum after 96 h, again indicating autophagy (Fig. 4A). Signs of autophagy were absent in LNCaP cells.

To confirm the involvement of apoptosis and autophagy in LNCaP and PC-3M cells, respectively, trypan blue-positive cells were counted after treatment with sorafenib A and z-VAD-fmk or 3-methyladenine, inhibitors of apoptosis and autophagy, respectively. In LNCaP cells, a significant reduction of trypan blue-positive cells was seen in the presence of z-VAD-fmk, thereby confirming the apoptotic nature of cell death in LNCaP cells. Adding an inhibitor of apoptosis to sorafenib A-treated PC-3M cells could not prevent cell death, whereas simultaneous treatment with sorafenib A and 3-methyladenine prevented the cells from dying (Fig. 4C). Taken together, these data indicate that the majority of the observed cell death in PC-3M cells treated with sorafenib A cannot be attributed to apoptosis, but instead is caused by autophagy.

**Palmitic acid suppresses the cytotoxicity of sorafenib A in cancer cells.** To examine whether the death-inducing effects of sorafenib A are in fact due to cellular depletion of fatty acids, LNCaP and PC-3M cells were incubated with sorafenib A in medium supplemented with exogenous palmitic acid and dead cells were counted by trypan blue staining. As illustrated by Fig. 5, palmitic acid reduced the percentage of dead cells from apparently 30% to 5% to 10% (similar to control levels), indicating that addition of palmitic acid almost completely rescues cells from sorafenib A-induced cell death. These effects were not caused by a reduction in the uptake or efficacy of sorafenib A. In fact, although palmitic acid reduced [<sup>2-14</sup>C]acetate incorporation in cellular lipids (as expected), sorafenib A reduced [<sup>2-14</sup>C]acetate incorporation to the same level as in the absence of palmitic acid (Fig. 5B). This indicates that the observed cell death in prostate cancer cells is caused by depletion of fatty acids.

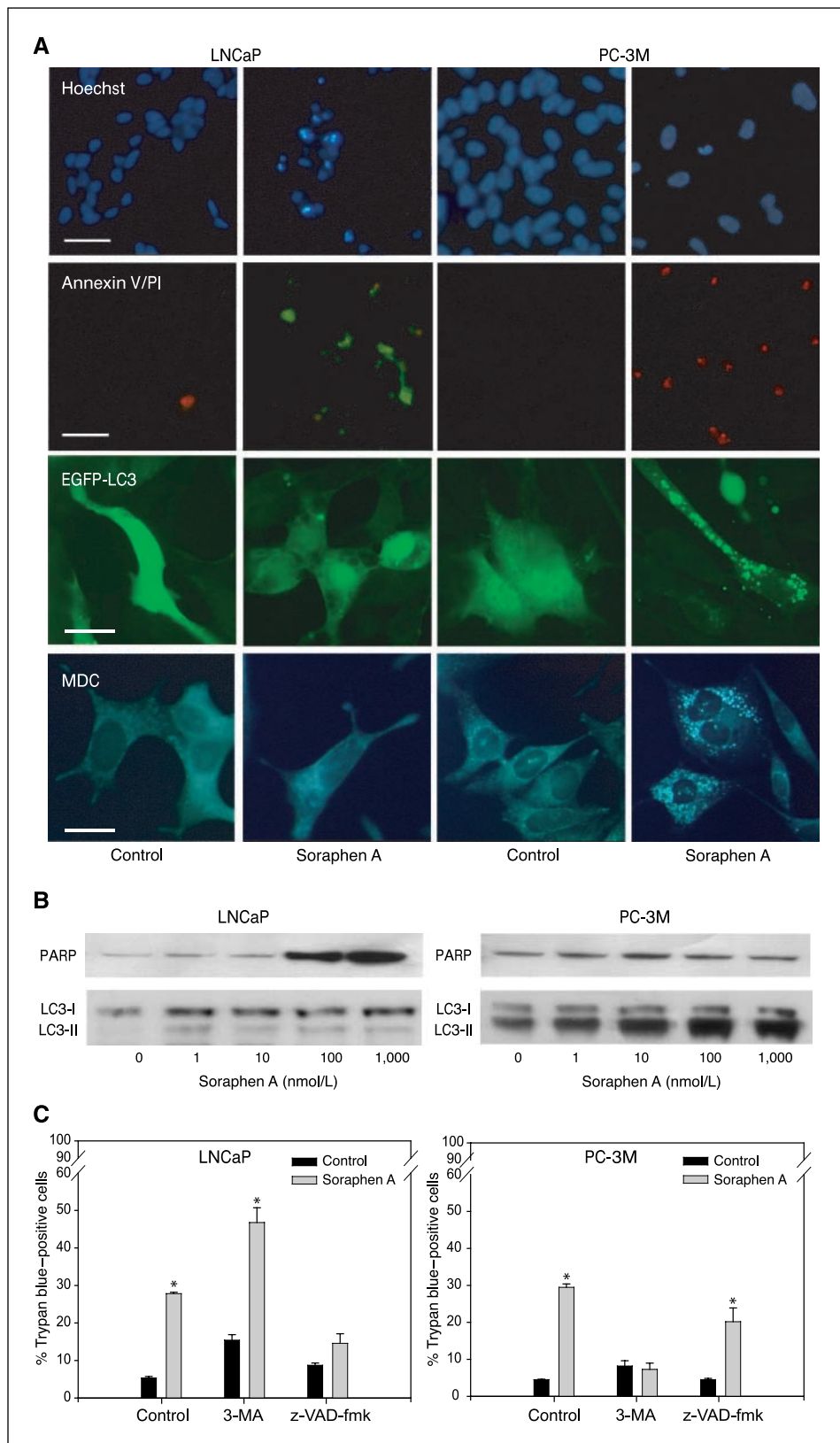
## Discussion

Here, we show that ACC activity plays a cardinal role in the lipid homeostasis of cancer cells. Treatment of LNCaP and PC-3M prostate cancer cells with sorafenib A, a highly powerful dual inhibitor of ACCs with a well-known and unique mechanism of action (31, 32), potentially inhibited lipid synthesis and increased fatty acid oxidation. Cells stopped proliferating and were arrested in the G<sub>0</sub>-G<sub>1</sub> phase of the cell cycle. A substantial fraction of the cells ultimately died. In LNCaP cells, sorafenib A activated the apoptosis program, whereas in PC-3M cells, cell death was associated with the induction of autophagy. Although it remains unclear why the two cancer cell lines died through different mechanisms, several lines of evidence point to a shortage of lipids as the main trigger of cell death: (a) cell death in both cell lines was accompanied by a significant decrease in the cellular levels of phospholipids; (b)

administration of exogenous palmitic acid completely rescued the cells from cell death; and (c) in the premalignant prostatic cell line BPH-1, which did not display a significant change in the cellular levels of phospholipids upon exposure to sorafenib, no induction

of cell death was observed. As dual inhibition of ACCs by sorafenib A blocks the formation of malonyl-CoA, these findings provide final evidence that a decrease in the cellular fatty acid supply per se may cause cancer cell death. These observations do not preclude that

**Figure 4.** Sorafenib A induces apoptosis in LNCaP cells and autophagy in PC-3M cells. **A**, cells were exposed to vehicle (control) or 100 nmol/L sorafenib A for 96 h as indicated. Afterward, cells were stained with Hoechst 33342, Annexin V-FITC, and propidium iodide (PI) or monodansylcadaverine (MDC) and analyzed by fluorescence microscopy. For analysis of the localization of LC3, cells were transfected with a plasmid pEGFP-LC3 6 h before sorafenib A treatment. Bars, 50  $\mu$ m. Results are representative of three independent experiments. **B**, immunoblot analysis of PARP and LC3. Cells were treated with sorafenib A as indicated. After 96 h of incubation, equal amounts of protein were subjected to immunoblot analysis with an antiserum against PARP or LC3. Equal loading of proteins was confirmed by immunoblotting for  $\alpha$ -tubulin (not shown). Results are representative of three independent experiments. **C**, cells were seeded in a 6-cm dish at a density of  $4 \times 10^5$  per dish (LNCaP) or  $1 \times 10^5$  per dish (PC-3M) and treated with 100 nmol/L sorafenib A or vehicle. Twenty-four hours later, z-VAD-fmk was added to the respective dishes. After 48 h of sorafenib A treatment, 3-methyladenine (3-MA) was added to the respective dishes. Ninety-six hours after sorafenib A treatment, cells were collected and stained with trypan blue. The percentage of dead cells was counted. Results are representative of three independent experiments. Columns, means of three values; bars, SE. \*,  $P < 0.05$ , significantly different from control (0 nmol/L).



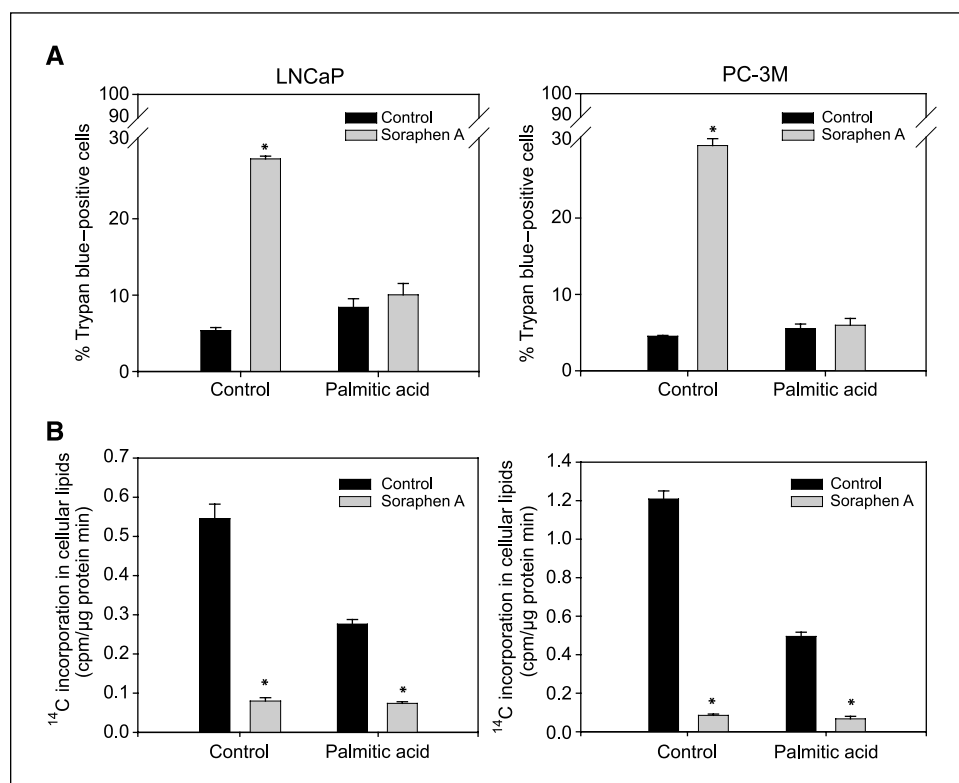


**Figure 5.** Palmitic acid suppresses the cytotoxicity of sorafenib A in cancer cells. **A**, cells were seeded in a 6-cm dish at a density of  $4 \times 10^5$  per dish (LNCaP) or  $1 \times 10^5$  per dish (PC-3M) and treated with 100 nmol/L sorafenib A or vehicle. Palmitic acid-BSA was added to the culture medium to a final concentration of 75  $\mu$ mol/L. After 96 h, cells were collected, stained with trypan blue, and the percentage of dead cells was counted. Results are representative of three independent experiments. Columns, means of three values; bars, SE. \*,  $P < 0.05$ , significantly different from control (0 nmol/L sorafenib A). **B**, cells were seeded and treated as in (A). After 20 h, cells were exposed to  $[2-^{14}\text{C}]$ acetate for 4 h. Cellular lipids were extracted and  $[2-^{14}\text{C}]$ acetate incorporation was measured by scintillation counting. Results are representative of two independent experiments. Columns, means of three values; bars, SE. \*,  $P < 0.05$ , significantly different from control (0 nmol/L sorafenib A).

increases in malonyl-CoA may also be involved in the mechanism of cell death induced by inhibition of FASN. They do, however, indicate that ACCs play an essential role in the lipid homeostasis in cancer cells and that, in addition to FASN, ACCs may also be attractive targets for antineoplastic intervention. One interesting observation in this respect is the differential sensitivity of the cancer cells and the premalignant cells to sorafenib A. Despite the fact that sorafenib A decreased  $[2-^{14}\text{C}]$ acetate incorporation in phospholipids in the premalignant cells, it did not evoke significant changes in the phospholipid content. Concomitantly, the proliferation and survival of premalignant cells were only marginally affected by the compound. The reason for this insensitivity remains poorly understood and is subject to further investigation. As BPH-1 and PC-3M proliferated at similar rates, the relative insensitivity of the premalignant cells cannot be explained merely by differences in growth rate. It is possible that the differential selectivity is caused by the somewhat lower rate of fatty acid oxidation in BPH-1 cells. An attractive alternative explanation is that cancer cells and premalignant cells exhibit differences in transporter-mediated uptake of exogenous lipids, providing a basis for cancer selective effects of ACC and FASN inhibitors. At high concentrations, the uptake of exogenous fatty acids becomes transporter independent, overriding differences in fatty acid uptake. This feature may also explain why no induction of cell death was seen previously with TOFA (23). TOFA is a fatty acid derivative that is rapidly metabolized in cancer cells and at high concentrations may even rescue cells from fatty acid depletion (43, 44). As serum levels of fatty acids in healthy individuals are even higher than those in medium used for supplementation, one might argue that ACC inhibitors would have no effect on cancer cells *in vivo*. Systemic administration of ACC inhibitors, however, is expected to decrease levels of circulating lipids (45). Perhaps more importantly, recent

findings have indicated that cancer cells express decreased levels of lipoprotein lipase (46). This would reduce the access of cancer cells to circulating lipids and provide another mechanism to render cancer tissue more prone to fatty acid depletion by ACC and FASN inhibitors than normal tissue. Although sorafenib A is a unique new tool to study the role of altered fatty acid metabolism in cancer cells, to test *in vivo* it would require a different pharmaceutical formulation due to its poor water solubility and its low bioavailability. With the recent surge of interest in this class of enzyme inhibitors also for other medical applications, including treatment of the metabolic syndrome (45, 47), new compounds may become available, allowing to test the concept of ACC inhibition for antineoplastic therapy.

In conclusion, to our knowledge, this is the first study showing that a chemical ACC inhibitor completely blocks fatty acid synthesis and decreases phospholipid levels in cancer cells. Inhibition is already evident at nanomolar concentrations and results in induction of cell death selectively in cancer cells, thereby further underscoring the potential of lipogenesis inhibition (and more in particular ACC inhibition) for future antineoplastic therapies.

## Acknowledgments

Received 2/5/2007; revised 4/25/2007; accepted 6/12/2007.

**Grant support:** Concerted Research Action Fund (K.U. Leuven); Research Foundation-Flanders; and Interuniversity Poles of Attraction Programme-Belgian State, Prime Minister's Office, Federal Office for Scientific, Technical and Cultural Affairs. L. Timmermans, K. Scheys, and K. Brusselmans are research assistants and a postdoctoral fellow, respectively, of the Research Foundation-Flanders.

The costs of publication of this article were defrayed in part by the payment of page charges. This article must therefore be hereby marked *advertisement* in accordance with 18 U.S.C. Section 1734 solely to indicate this fact.

We thank P.P. Van Veldhoven for the quantitation of phospholipids and free cholesterol.

## References

1. Swinnen JV, Brusselmans K, Verhoeven G. Increased lipogenesis in cancer cells: new players, novel targets. *Curr Opin Clin Nutr Metab Care* 2006;9:358–65.
2. Kuhajda FP. Fatty acid synthase and cancer: new application of an old pathway. *Cancer Res* 2006;66:5977–80.
3. Wakil SJ, Stoops JK, Joshi VC. Fatty acid synthesis and its regulation. *Annu Rev Biochem* 1983;52:537–79.
4. Milgraum LZ, Witters LA, Pasternack GR, Kuhajda FP. Enzymes of the fatty acid synthesis pathway are highly expressed in *in situ* breast carcinoma. *Clin Cancer Res* 1997;3:2115–20.
5. Swinnen JV, Vanderhoydonc F, Elgmal AA, et al. Selective activation of the fatty acid synthesis pathway in human prostate cancer. *Int J Cancer* 2000;88:176–9.
6. Piyathilake CJ, Frost AR, Manne U, et al. The expression of fatty acid synthase (FASE) is an early event in the development and progression of squamous cell carcinoma of the lung. *Hum Pathol* 2000;31:1068–73.
7. Swinnen JV, Roskams T, Joniau S, et al. Overexpression of fatty acid synthase is an early and common event in the development of prostate cancer. *Int J Cancer* 2002; 98:19–22.
8. Kuhajda FP. Fatty-acid synthase and human cancer: new perspectives on its role in tumor biology. *Nutrition* 2000;16:202–8.
9. Pizer ES, Jackisch C, Wood FD, Pasternack GR, Davidson NE, Kuhajda FP. Inhibition of fatty acid synthesis induces programmed cell death in human breast cancer cells. *Cancer Res* 1996;56:2745–7.
10. Pizer ES, Wood FD, Heine HS, Romantsev FE, Pasternack GR, Kuhajda FP. Inhibition of fatty acid synthesis delays disease progression in a xenograft model of ovarian cancer. *Cancer Res* 1996;56:1189–93.
11. Pizer ES, Chrest FJ, DiGiuseppe JA, Han WF. Pharmacological inhibitors of mammalian fatty acid synthase suppress DNA replication and induce apoptosis in tumor cell lines. *Cancer Res* 1998;58:4611–5.
12. Kuhajda FP, Pizer ES, Li JN, Mani NS, Frehywot GL, Townsend CA. Synthesis and antitumor activity of an inhibitor of fatty acid synthase. *Proc Natl Acad Sci U S A* 2000;97:3450–4.
13. Li JN, Gorospe M, Chrest FJ, et al. Pharmacological inhibition of fatty acid synthase activity produces both cytostatic and cytotoxic effects modulated by p53. *Cancer Res* 2001;61:1493–9.
14. Brusselmans K, De Schrijver E, Heyns W, Verhoeven G, Swinnen JV. Epigallocatechin-3-gallate is a potent natural inhibitor of fatty acid synthase in intact cells and selectively induces apoptosis in prostate cancer cells. *Int J Cancer* 2003;106:856–62.
15. Kridel SJ, Axelrod F, Rozenkrantz N, Smith JW. Orlistat is a novel inhibitor of fatty acid synthase with antitumor activity. *Cancer Res* 2004;64:2070–5.
16. De Schrijver E, Brusselmans K, Heyns W, Verhoeven G, Swinnen JV. RNA interference-mediated silencing of the fatty acid synthase gene attenuates growth and induces morphological changes and apoptosis of LNCaP prostate cancer cells. *Cancer Res* 2003;63: 3799–804.
17. Abu-Elheiga L, Jayakumar A, Baldini A, Chirala SS, Wakil SJ. Human acetyl-CoA carboxylase: characterization, molecular cloning, and evidence for two isoforms. *Proc Natl Acad Sci U S A* 1995;92:4011–5.
18. Widmer J, Fassihi KS, Schlichter SC, et al. Identification of a second human acetyl-CoA carboxylase gene. *Biochem J* 1996;316:915–22.
19. Carretero J, Medina PP, Blanco R, et al. Dysfunctional AMPK activity, signalling through mTOR and survival in response to energetic stress in LKB1-deficient lung cancer. *Oncogene* 2007;26:1616–25.
20. Shaw RJ, Kosmatka M, Bardeesy N, et al. The tumor suppressor LKB1 kinase directly activates AMP-activated kinase and regulates apoptosis in response to energy stress. *Proc Natl Acad Sci U S A* 2004;101:3329–35.
21. Moreau K, Dizin E, Ray H, et al. BRCA1 affects lipid synthesis through its interaction with acetyl-CoA carboxylase. *J Biol Chem* 2006;281:3172–81.
22. Magnard C, Bachelier R, Vincent A, et al. BRCA1 interacts with acetyl-CoA carboxylase through its tandem of BRCT domains. *Oncogene* 2002;21:6729–39.
23. Pizer ES, Thupari J, Han WF, et al. Malonyl-coenzyme-A is a potential mediator of cytotoxicity induced by fatty-acid synthase inhibition in human breast cancer cells and xenografts. *Cancer Res* 2000;60: 213–8.
24. Thupari JN, Pinn ML, Kuhajda FP. Fatty acid synthase inhibition in human breast cancer cells leads to malonyl-CoA-induced inhibition of fatty acid oxidation and cytotoxicity. *Biochem Biophys Res Commun* 2001; 285:217–23.
25. Brusselmans K, De Schrijver E, Verhoeven G, Swinnen JV. RNA interference-mediated silencing of the acetyl-CoA-carboxylase- $\alpha$  gene induces growth inhibition and apoptosis of prostate cancer cells. *Cancer Res* 2005;65:6719–25.
26. Chajes V, Cambot M, Moreau K, Lenoir GM, Joulin V. Acetyl-CoA carboxylase  $\alpha$  is essential to breast cancer cell survival. *Cancer Res* 2006;66:5287–94.
27. Bedorf N, Schomburg D, Gerth K, Reichenbach H, Höfle G. Isolation and structure elucidation of soraphen A1, a novel antifungal macrolide from *Sorangium cellulosum*. *Liebigs Ann Chem* 1993;1017–21.
28. Gerth K, Bedorf N, Irschik H, Höfle G, Reichenbach H. The soraphens: a family of novel antifungal compounds from *Sorangium cellulosum* (Myxobacteria). I. Soraphen A1  $\alpha$ : fermentation, isolation, biological properties. *J Antibiot (Tokyo)* 1994;47:23–31.
29. Pridzun L, Sasse F, Reichenbach H. Inhibition of fungal acetyl-CoA carboxylase: A novel target discovered with the myxobacterial compound soraphen. In: Dixon GK, Copping LG, Hollomon DW, editors. *Antifungal agents*. Oxford: BIOS Scientific Publishers Ltd.; 1995. p. 99–109.
30. Vahlensieck HF, Pridzun L, Reichenbach H, Hinnen A. Identification of the yeast ACC1 gene product (acetyl-CoA carboxylase) as the target of the polyketide fungicide soraphen A. *Curr Genet* 1994;25:95–100.
31. Shen Y, Volrath SL, Weatherly SC, Elich TD, Tong L. A mechanism for the potent inhibition of eukaryotic acetyl-coenzyme A carboxylase by soraphen A, a macrocyclic polyketide natural product. *Mol Cell* 2004; 16:881–91.
32. Weatherly SC, Volrath SL, Elich TD. Expression and characterization of recombinant fungal acetyl-CoA carboxylase and isolation of a soraphen-binding domain. *Biochem J* 2004;380:105–10.
33. Swinnen JV, Van Veldhoven PP, Esquet M, Heyns W, Verhoeven G. Androgens markedly stimulate the accumulation of neutral lipids in the human prostatic adenocarcinoma cell line LNCaP. *Endocrinology* 1996; 137:4468–74.
34. Van Veldhoven PP, Bell RM. Effect of harvesting methods, growth conditions and growth phase on diacylglycerol levels in cultured human adherent cells. *Biochim Biophys Acta* 1988;959:185–96.
35. Van Veldhoven PP, Meyhi E, Mannaerts GP. Enzymatic quantitation of cholesterol esters in lipid extracts. *Anal Biochem* 1998;258:152–5.
36. Kabeya Y, Mizushima N, Ueno T, et al. LC3, a mammalian homologue of yeast Apg8p, is localized in autophagosome membranes after processing. *EMBO J* 2000;19:5720–8.
37. Biederbick A, Kern HF, Elsasser HP. Monodansylcadaverine (MDC) is a specific *in vivo* marker for autophagic vacuoles. *Eur J Cell Biol* 1995;66:3–14.
38. Niemann A, Takatsuki A, Elsasser HP. The lysosomotropic agent monodansylcadaverine also acts as a solvent polarity probe. *J Histochem Cytochem* 2000;48: 251–8.
39. Munafò DB, Colombo MI. A novel assay to study autophagy: regulation of autophagosome vacuole size by amino acid deprivation. *J Cell Sci* 2001;114:3619–29.
40. Kiorpes TC, Hoerr D, Ho W, Weaner LE, Inman MG, Tutwiler GF. Identification of 2-tetradecylglycidyl coenzyme A as the active form of methyl 2-tetradecylglycidate (methyl palmoixirate) and its characterization as an irreversible, active site-directed inhibitor of carnitine palmitoyltransferase A in isolated rat liver mitochondria. *J Biol Chem* 1984;259:9750–5.
41. Swinnen JV, Van Veldhoven PP, Timmermans L, et al. Fatty acid synthase drives the synthesis of phospholipids partitioning into detergent-resistant membrane microdomains. *Biochem Biophys Res Commun* 2003; 302:898–903.
42. Swinnen JV, Verhoeven G. Androgens and the control of lipid metabolism in human prostate cancer cells. *J Steroid Biochem Mol Biol* 1998;65:191–198.
43. Halvorson DL, McCune SA. Inhibition of fatty acid synthesis in isolated adipocytes by 5-(tetradecyloxy)-2-furoic acid. *Lipids* 1984;19:851–856.
44. Otto DA, Chatzidakis C, Kasziba E, Cook GA. Reciprocal effects of 5-(tetradecyloxy)-2-furoic acid on fatty acid oxidation. *Arch Biochem Biophys* 1985;242: 23–31.
45. Harwood HJ, Jr. Treating the metabolic syndrome: acetyl-CoA carboxylase inhibition. *Expert Opin Ther Targets* 2005;9:267–81.
46. Kinlaw WB, Quinn JL, Wells WA, Roser-Jones C, Moncur JT. Spot 14: A marker of aggressive breast cancer and a potential therapeutic target. *Endocrinology* 2006; 147:4048–55.
47. Harwood HJ, Jr. Acetyl-CoA carboxylase inhibition for the treatment of metabolic syndrome. *Curr Opin Investig Drugs* 2004;5:283–9.